

Reducing pulse distortion in fast-light pulse propagation through an erbium-doped fiber amplifier

Heedeuk Shin, Aaron Schweinsberg, George Gehring, Katie Schwertz, Hye Jeong Chang,* and Robert W. Boyd

The Institute of Optics, University of Rochester, Rochester, New York 14627, USA

Q-Han Park

Department of Physics, Korea University, Seoul, 136-701, Korea

Daniel J. Gauthier

Department of Physics, Duke University, Durham, North Carolina 27708, USA

Received December 22, 2006; accepted January 2, 2007;
posted January 25, 2007 (Doc. ID 78405); published March 19, 2007

When a pulse superposed on a cw background propagates through an erbium-doped fiber amplifier with a negative group velocity, either pulse broadening or pulse compression can be observed. These effects can be explained in terms of two competing mechanisms: gain recovery and pulse spectrum broadening. The distortion of the pulse shape caused by these effects depends on input pulse width, pump power, and background-to-pulse power ratio. With the proper choice of these three parameters, we can obtain significant pulse advancement with minimal pulse distortion. © 2007 Optical Society of America
OCIS codes: 190.5530, 060.2410.

The use of controllable slow- and fast-light pulse propagation through material systems has been of recent interest to the telecommunications and information processing communities.^{1,2} Since distortion can compromise the information content of a stream of pulses, distortion reduction mechanisms are particularly important. Several investigations have been concerned with pulse-distortion compensation in slow- and fast-light systems using multiple gain lines or phase masks.³⁻⁶

Recently, we observed pulse compression⁷ as well as pulse broadening⁸ in an erbium-doped fiber amplifier (EDFA) by about 10% of the pulse width in each case. In both cases, the amplifier was operated in the fast-light regime with fast-light propagation occurring as a consequence of coherent population oscillations (CPOs). The intent of this Letter is to investigate the mechanisms responsible for the pulse broadening and compression and to demonstrate that distortion can be minimized while maintaining significant pulse advancement.

Fast light by CPOs occurs in the nonlinear regime, i.e., when the signal power is comparable with or greater than the saturation power of the medium. In such cases, pulse broadening and compression can be described in terms of two competing mechanisms. Pulse broadening is caused by a time-dependent saturation of the amplifier gain. Without any background, the amplifier gain is quickly depleted by the leading edge of a pulse, but a strong applied pump field can re-excite the medium. This *gain recovery* occurs over a characteristic time that depends on both the lifetime of the metastable state and the applied pump intensity. If the input pulse duration is compa-

rable with or longer than the gain recovery time, the trailing edge of the pulse may experience this recovered gain, broadening the pulse.⁹

Pulse compression, on the other hand, can be induced by superposing a pulse on a cw background that is larger than the saturation intensity of the EDFA ($I_{\text{sat}} \sim 3 \text{ kW/cm}^2$ at 1550 nm). In this case, CPOs create a narrow hole in the EDFA gain profile and thus produces anomalous dispersion. As a result, the wings of the pulse spectrum experience a larger gain than the central frequency components, thereby broadening the pulse spectrum and compressing the pulse in the time domain. Cao *et al.* explained this pulse compression with the negative second derivative of the absorption coefficient and derived the pulse compression and the advancement factors.¹⁰ This mechanism, which we refer to as *pulse spectrum broadening*, competes with gain recovery. By controlling these two mechanisms, we can regulate the amount of broadening or compression experienced by a pulse during propagation through an amplifier.

To examine the advancement and distortion effects, we have performed experiments using the setup illustrated in Fig. 1. We use a tunable 1550 nm diode laser and an electro-optic modulator (EOM) to generate a Gaussian pulse on a variable-intensity background. Two percent of this signal beam is split off for use as a reference, while the rest is sent into an EDFA that is pumped by a copropagating field from a 980 nm diode laser. The output pulse is measured after filtering out the pump using a wavelength division multiplexer (WDM). Furthermore, to model our experimental observations, we perform computer simulations of pulse propagation through

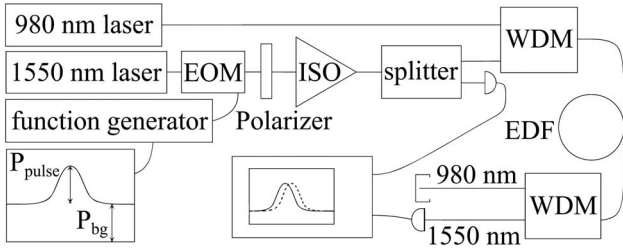


Fig. 1. Experimental setup. The signal beam is sent through an isolator and coupled into a fiber. The pump beam at 980 nm and the signal beam at 1550 nm are combined at a WDM and copropagate through the EDFA. P_{pulse} and P_{bg} represent the power of the pulse and the background, respectively.

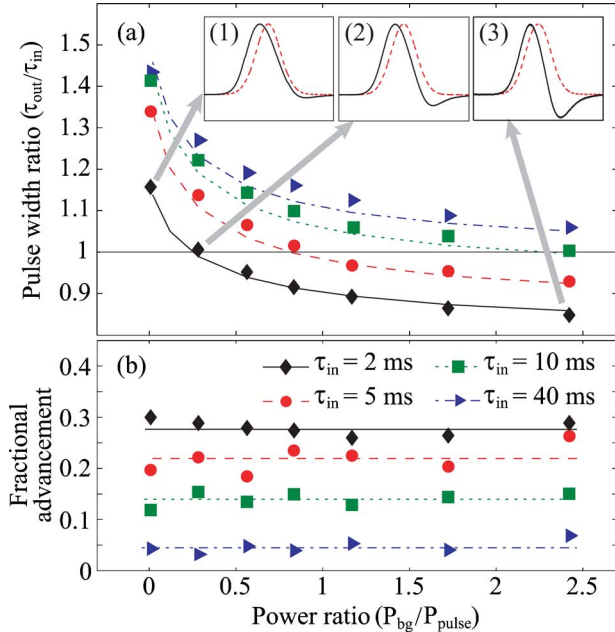


Fig. 2. (Color online) (a) Experimentally measured (symbols) and theoretically predicted (curves) pulse-width ratio versus background-to-pulse power ratio for different pulse widths. The horizontal line at the pulse-width ratio of 1 represents no pulse-width distortion. Inset: experimentally measured input (dashed curve) and output (solid curve) pulse waveforms illustrate distortion accompanied by (1) broadening, (2) no pulse-width distortion, and (3) compression. (b) Experimentally measured (symbols) and averaged (lines) fractional advancement versus background-to-pulse power ratio.

the EDFA by numerically solving the five-level-system rate equations for erbium ions, including amplified spontaneous emission¹¹ (ASE).

To characterize pulse-width distortion, which is pulse broadening or compression, we define the pulse-width ratio as the ratio of the output pulse full width at half-maximum (FWHM) to the input pulse FWHM ($\tau_{\text{out}}/\tau_{\text{in}}$). Another important parameter is the background-to-pulse power ratio ($P_{\text{bg}}/P_{\text{pulse}}$). In Fig. 2(a), we plot the pulse-width ratio against the background-to-pulse power ratio for various input pulse widths. The pump power P_{pump} and pulse power P_{pulse} are 35 mW and 55 μ W, respectively, and the average inversion level, $N_e - N_g/N_e = 0.9$, where N_e and N_g are the number density of erbium ions in the EDFA. Under our experimental conditions, pulse-

width ratios between 0.84 and 1.43 were observed for different pulse widths and background-to-pulse power ratios. The experimental results are well described by the numerical model. However, fractional advancement, the ratio of pulse advancement to input pulse FWHM, was found to be independent of the power ratio as shown in Fig. 2(b). Therefore we conclude that the power ratio can be used as a free parameter to minimize the pulse distortion without changing the fractional advancement. The output pulse width is equal to the input pulse width when the background-to-pulse power ratio is about 0.3, 0.8, and 2.4 for pulse widths of 2, 5, and 10 ms, respectively.

In addition, the time traces of the input and output pulse for 2 ms pulse width are shown in insets (1), (2), and (3) of Fig. 2 at power ratios of 0, 0.8, and 2.5, respectively. Pulse broadening due to the gain recovery effect occurs at low background-to-pulse power ratio as shown in inset (1) of Fig. 2, while inset (3) illustrates that a higher background-to-pulse power ratio is associated with a smaller gain recovery effect and larger pulse spectrum broadening, resulting in a tendency toward pulse compression. Furthermore, the broadening effect for 2 ms pulse width is weaker than that for longer pulse widths, since the pulse tail exits the material too quickly to experience the recovered gain. The dip in the tail of the output pulse of inset (1) of Fig. 2 is caused by the reduced ASE. Note that the pulse widths of the input and output pulses are equal for a background-to-pulse power ratio of 0.3 as shown in inset (2) of Fig. 2, which indicates that the pulse-width distortion is eliminated by controlling the power ratio.

Even though the pulse-width distortion is removed, the trailing edge of the pulse of inset (2) of Fig. 2 illustrates additional pulse-shape distortion. The degree of this distortion can be characterized by the quantity¹²

$$D = \left(\frac{\int_{-\infty}^{+\infty} ||E'(t + \Delta t)|^2 - |E(t)|^2| dt}{\int_{-\infty}^{+\infty} |E'(t + \Delta t)|^2 dt} \right)^{1/2} - \left(\frac{\int_{-\infty}^{+\infty} ||E(t + \delta t)|^2 - |E(t)|^2| dt}{\int_{-\infty}^{+\infty} |E'(t + \delta t)|^2 dt} \right)^{1/2}, \quad (1)$$

where $E'(t)$ and $E(t)$ are the normalized output and input field envelopes, respectively, Δt is the time advancement of the pulse, and δt is the temporal resolution of our detection system. The first term represents the distortion caused by pulse reshaping, and the second term is a measure of noise. Figure 3 shows a distinct pattern in both the experimental and numerical data. At low power ratios, the primary source of distortion is pulse broadening associated with gain recovery, leading to the behavior shown in inset (1) of Fig. 2. However, once the power ratio becomes higher

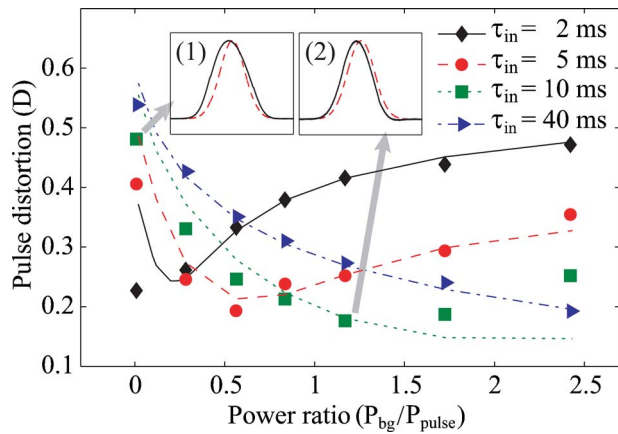


Fig. 3. (Color online) Experimentally measured (symbols) and theoretically predicted (curves) pulse-shape distortion versus background-to-pulse power ratio for different pulse widths. Inset: experimentally measured input (dashed curve) and output (solid curve) pulse waveforms of 10 ms pulse width at power ratios of (1) 0 and (2) 1.2, respectively.

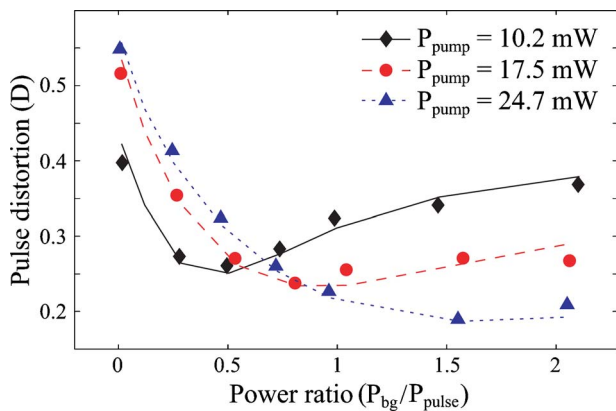


Fig. 4. (Color online) Experimentally measured (symbols) and theoretically predicted (curves) pulse distortion versus background-to-pulse power ratio for different pump powers.

than the minimum distortion point, pulse compression becomes the dominant contribution to the distortion, leading to the behavior shown in inset (3) of Fig. 2. To emphasize the possibility of reducing pulse-shape distortion, time traces of the input and output pulse for 10 ms pulse widths at power ratios of 0 and 1.2 are shown in insets (1) and (2) of Fig. 3. Note that the 10 ms output pulse at zero power ratio shows a stronger pulse broadening effect than that of the 2 ms pulse width in inset (1) of Fig. 2. In addition, the input and output pulse shapes at a power ratio of 1.2, which is approximately the minimum distortion point, show pulse advancement with little distortion. Thus proper selection of the power ratio for a particular pulse width can reduce pulse distortion.

Furthermore, we investigated the dependence of pulse distortion on pump power because the process of gain recovery is pump power dependent. The pulse

power and the pulse width were held fixed at 80 μ W and 10 ms, respectively, while the average inversion level was about 0.86, 0.79, and 0.54 for the pump powers of 10.2, 17.5, and 24.7 mW, respectively. These results are shown in Fig. 4. The gain recovery becomes stronger if the pump power increases and compensates for the pulse spectrum broadening at the higher background-to-pulse power ratios. The fractional advancement of a Gaussian pulse of 10 ms pulse width is largest when the pump power is 17.5 mW, agreeing very well with Ref. 8, and has no significant dependence on the power ratio.

In conclusion, we observed pulse broadening and compression effects in fast-light propagation through an EDFA. These results can be interpreted by examining the competing mechanisms of gain recovery and pulse spectrum broadening. We found that distortion depends on pulse width, pump power, and background-to-pulse power ratio and that under many conditions pulse distortion effects can be minimized by adding a background of appropriate power. With a 10 ms pulse width, significant fractional advancement (~ 0.17) and minimal distortion was obtained for a background-to-pulse power ratio of about 0.75 and a pump power of 17.5 mW.

We gratefully acknowledge discussions with Govind Agrawal. This work was supported by Korea Research Foundation (KRF) and their Post-doctoral Fellowship program, NSF grant ECS-0355206, and the DARPA/DSO Slow Light program. R. W. Boyd's e-mail address is boyd@optics.rochester.edu.

*Present address, The Korean Intellectual Property Office, DaeJeon 302-791, Korea.

References

1. R. W. Boyd, D. J. Gauthier, and A. L. Gaeta, *Opt. Photon. News* **17**(4), 18 (2006).
2. R. W. Boyd and D. J. Gauthier, *Nature* **441**, 701 (2006).
3. D. Eliyahu, R. A. Salvatore, J. Rosen, A. Yariv, and J. Drolet, *Opt. Lett.* **20**, 1412 (1995).
4. M. D. Stenner, M. A. Neifeld, Z. Zhu, A. M. C. Dawes, and D. J. Gauthier, *Opt. Express* **13**, 9995 (2005).
5. K. Y. Song, M. Gonzalez Herraes, and L. Thevenaz, *Opt. Express* **13**, 9758 (2005).
6. R. Pant, M. D. Stenner, M. A. Neifeld, Z. Shi, R. W. Boyd, and D. J. Gauthier, "Maximizing the opening of eye diagrams for slow-light systems" (submitted to *J. Lightwave Technol.*).
7. G. M. Gehring, A. Schweinsberg, C. Barsi, N. Kostinski, and R. W. Boyd, *Science* **312**, 895 (2006).
8. A. Schweinsberg, N. N. Lepeshkin, M. S. Bigelow, R. W. Boyd, and S. Jarabo, *Europhys. Lett.* **73**, 218 (2006).
9. G. P. Agrawal and N. A. Olsson, *IEEE J. Quantum Electron.* **25**, 2297 (1989).
10. H. Cao, A. Dogariu, and L. J. Wang, *IEEE J. Sel. Top. Quantum Electron.* **9**, 52 (2003).
11. P. F. Wysocki, J. L. Wagener, M. J. F. Digonnet, and H. J. Shaw, *Proc. SPIE* **1789**, 66 (1992).
12. M. S. Bigelow, N. N. Lepeshkin, H. Shin, and R. W. Boyd, *J. Phys. Condens. Matter* **18**, 3117 (2006).